International Journal of Heat and Technology
Vol. 44, No. 1, February, 2026, pp. 260-268
Journal homepage: http://iieta.org/journals/ijht

Role of Pigment Volume Concentration in Controlling Optical Properties and Cooling Performance of Radiative Coatings

Mohammad Alexin Putra, Muhammad Fuad Abdul Hakim, Diki Ismail Permana*

Department of Mechanical Engineering, Faculty of Industrial Technology, Institut Teknologi Nasional Bandung, Bandung 40124, Indonesia

Corresponding Author Email: dicky91permana@itenas.ac.id

https://doi.org/10.18280/ijht.440123

Received: 23 October 2025
Revised: 12 February 2026
Accepted: 20 February 2026
Available online: 28 February 2026

Keywords:
radiative cooling paint, pigment volume concentration, thermal management, surface temperature reduction, optical properties, coating durability, passive cooling, pigment optimization

ABSTRACT

Radiative cooling paint (RCP) provides a passive method for managing heat. It reflects solar radiation and emits heat using infrared radiation. The pigment volume concentration (PVC) primarily governs RCP's performance, striking a balance between thermal behavior and mechanical strength. This study investigates the impact of PVC on temperature reduction and surface cracking in RCP. Twenty-five samples were prepared with five pigment types: calcium carbonate ($CaCO_3$), barium sulfate ($BaSO_4$), magnesium oxide (MgO), titanium dioxide (TiO_2), and silicon dioxide (SiO_2) at five PVC levels: 40%, 50%, 60%, 70%, and 80%. Each formulation was applied to an aluminum substrate measuring 100 mm × 100 mm × 2 mm, with a coating thickness of 400 µm. Researchers examined surface cracking and tested the temperature decrease under direct sunlight for about five hours. Results show that the optimal PVC is 60% for $CaCO_3$, $BaSO_4$, MgO, and TiO_2, and 40% for SiO_2. The average temperature reductions for each concentration are 6.3 °C, 6.6 °C, 3.8 °C, 4.2 °C, and 5.4 °C, respectively. Most cracks appear at an 80% PVC level. These findings emphasize the importance of selecting the optimal pigment concentration to strike a balance between cooling and durability. This offers valuable insight into developing high-performance RCP for thermal regulation.

1. INTRODUCTION

The need for cooling is a crucial aspect of daily life, especially in indoor environments exposed to direct sunlight. A common example is the use of air conditioners (AC) to reduce indoor air temperature in buildings with sun-exposed roofs. To date, AC systems remain the primary choice for cooling indoor spaces [1]. However, such systems require significant external energy input, primarily in the form of electricity, and are therefore categorized as active cooling technologies. In contrast, passive cooling technologies have been developed to provide cooling effects without external energy input [2]. These technologies offer potential energy savings by reducing the demand for active cooling, thereby contributing to lower energy consumption and mitigating the environmental impacts associated with conventional cooling systems. Moreover, passive cooling can play a role in mitigating the effects of climate change associated with the extensive use of energy-intensive cooling devices [3].

Passive cooling technologies include phase change materials (PCMs) [4], heat sinks [5], evaporative cooling systems [6], and radiative cooling [7]. PCMs function by absorbing and storing heat during phase transitions, utilizing latent heat to maintain temperature stability. Heat sinks operate by transferring heat via conduction from a heat source and dissipating it to the surrounding air through convection. Evaporative cooling relies on the evaporation of water to increase humidity and lower air temperature. Another emerging passive cooling approach is radiative cooling, which operates by reflecting incoming solar radiation while emitting thermal radiation from the surface into outer space through the atmospheric window. This dual mechanism enables temperature reduction without external power input, as illustrated in Figure 1.

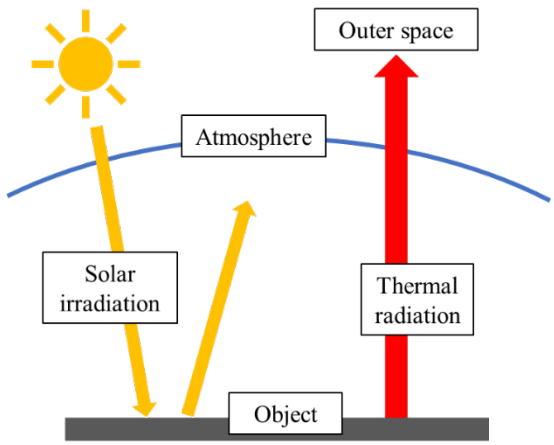

Figure 1. Simple schematic of radiative cooling

Recent research on radiative cooling has primarily focused on developing surface coatings capable of providing radiative

cooling effects, one of which is paint-based technology known as radiative cooling paint (RCP) [8]. RCP reduces the temperature of coated surfaces by simultaneously emitting thermal radiation and reflecting incoming solar irradiation. Generally, RCP formulations comprise three primary components: pigments, binders, and solvents. Pigments provide colour while determining the coating's solar reflectivity and thermal emissivity within the atmospheric window. The binder acts as a matrix that holds the pigment particles together and adheres them to the substrate, whereas the solvent serves as a medium to dissolve or disperse the binder and evaporates during the drying process.

A key performance indicator of RCP is its temperature decrease capability, defined as the temperature difference between an RCP-coated surface and an uncoated one under identical conditions. This performance is influenced by both the type of pigment and the pigment volume concentration (PVC). PVC, expressed as a percentage, represents the ratio of the pigment volume to the total solid volume (pigment plus binder) in the coating formulation [9]. While a higher PVC increases the number of pigment particles, thereby enhancing solar reflectivity and thermal emissivity, it simultaneously reduces the binder content. Insufficient binder weakens the matrix structure and may lead to cracking or poor mechanical integrity of the coating [10]. Previous studies have typically evaluated the temperature decrease performance of RCP using a single PVC value, as summarised in Table 1. However, a systematic investigation of the relationship between PVC and both cooling performance and coating durability remains limited. This research aims to address this gap by determining the optimal pigment concentration that maximises temperature reduction while preventing cracking in RCP formulations.

Table 1. Literature study of PVC

Study	Pigment	PVC
[11]	Calcium carbonate	60%
[12]	Calcium carbonate	50%
[13]	Calcium carbonate	70%
[14]	Barium sulfate	60%
[15]	Barium sulfate	60%
[16]	Magnesium oxide	65%
[17]	Titanium oxide	30%
[18]	Titanium oxide	15%
[19]	Silicon dioxide	35%

The use of a single PVC value in previous studies provides only a limited understanding of how pigment concentration influences the temperature decrease performance of RCP. Therefore, further investigation is necessary to evaluate the trends associated with increasing or decreasing PVC and their effects on both cooling performance and the formation of cracks in the RCP layer. By systematically varying the PVC, these relationships can be more clearly identified, enabling the determination of an optimal concentration that balances thermal performance and coating integrity. Accordingly, this study aims to determine the optimal PVC at which the RCP layer exhibits no cracking after drying while achieving the maximum temperature reduction.

2. MATERIALS AND METHODS

To determine the optimal PVC, RCP samples were prepared with different PVCs. A reference point of 60% PVC was chosen, following the formulation reported in a previous study [15]. PVC values were then adjusted above and below this reference to create five concentration levels: 40%, 50%, 60%, 70%, and 80%. PVC is defined as the volume ratio of pigment to binder in the RCP formulation. For example, a PVC of 40% means that the pigment makes up 40% of the total solid volume, while the remaining 60% consists of binder. The optimal PVC was identified based on two criteria: (1) no visible cracks on the dried RCP surface and (2) the highest temperature decrease achieved during testing.

The optimal PVC values were experimentally determined for five pigment types: calcium carbonate ($CaCO_3$), barium sulfate ($BaSO_4$), magnesium oxide (MgO), titanium dioxide (TiO_2), and silicon dioxide (SiO_2). These pigments were selected based on their frequent use in previous radiative cooling studies and their distinct optical properties—specifically, high solar reflectance and strong infrared emissivity. The binder was polymethyl methacrylate (PMMA), chosen for its transparency and good film-forming capability. Dimethylformamide (DMF) was used as the solvent due to its high solubility for PMMA and a suitable evaporation rate. The optimal PVC (X%) for each pigment is shown in Figure 2.

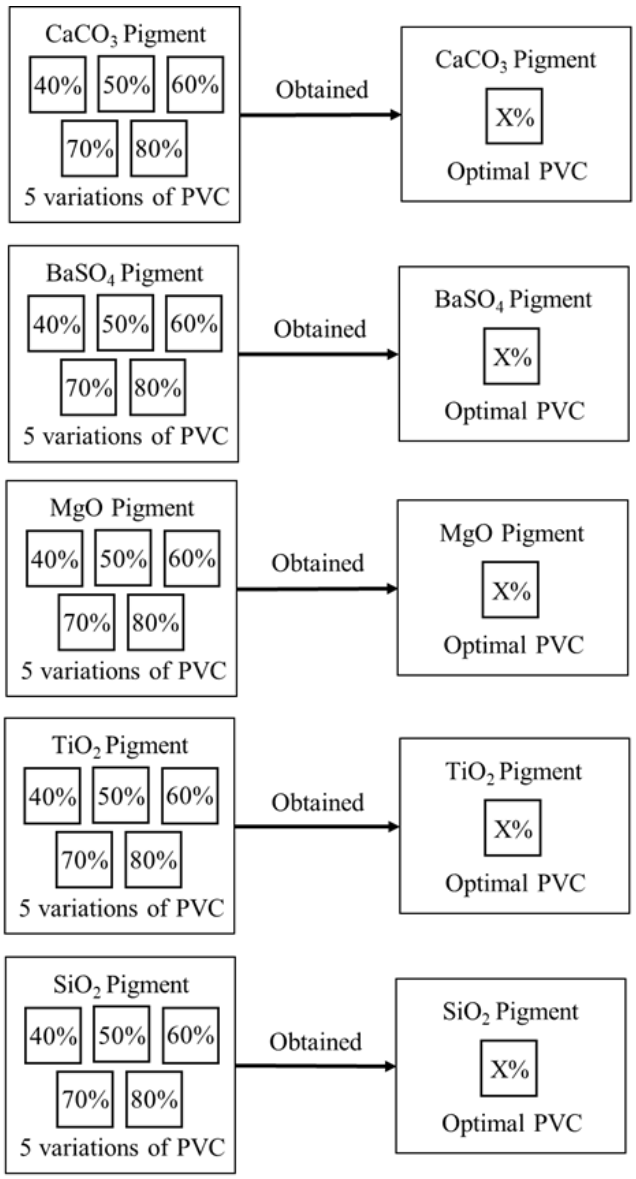

Figure 2. Test flow diagram of optimal PVC

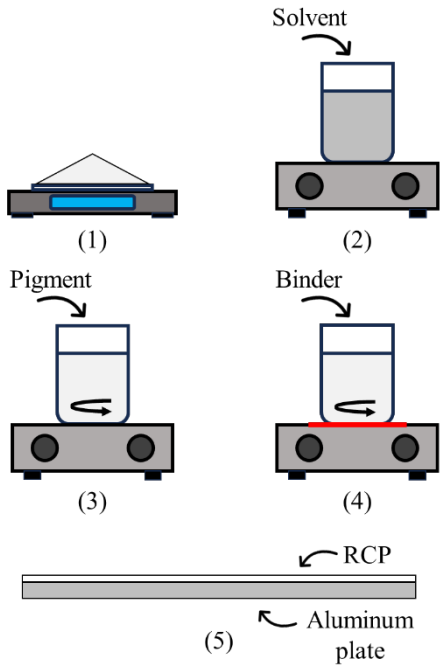

Figure 3. Steps for preparation of RCP samples: (1) weighing of materials, (2) addition of solvent, (3) addition of pigment, (4) addition of binder, (5) application on aluminum plate

Twenty-five RCP samples, consisting of five types of pigments and five variations of PVC, were prepared. The RCP samples were prepared, as shown in Figure 3. First, the pigment, binder, and solvent were weighed according to the specified PVC. PVC provides the volume ratio between the pigment and binder, but both materials are commercially available in solid form, so this volume ratio must be converted into a mass ratio using Eq. (1).

$$\frac{m_P}{m_B} = \frac{\rho_P \cdot PVC}{\rho_B \cdot (1 - PVC)}, \quad (1)$$

where, m_p and m_B represent the masses of the pigment and binder, respectively, while ρ_p and ρ_B denote their corresponding densities. The solvent amount was adjusted based on the binder mass, maintaining an initial binder-to-solvent mass ratio of 1:10. The preparation process began by placing the solvent in a beaker positioned on a hot plate stirrer. The pigment was gradually added to the solvent under continuous stirring to ensure uniform dispersion and prevent particle agglomeration. Subsequently, the binder was slowly introduced into the mixture and stirred until it was completely dissolved, yielding a homogeneous RCP solution ready for coating.

A total of 25 RCP samples were prepared, encompassing five pigment types and five PVC variations. Each formulation was applied onto an aluminum substrate measuring 100 mm × 100 mm × 2 mm, with an average coating thickness of approximately 400 µm. After drying, the coatings were visually inspected for surface cracking. The samples were then tested under direct sunlight to evaluate the temperature decrease for each pigment type and identify the PVC level that produced the highest cooling performance.

Aluminum plates were selected as substrates due to their favorable thermal properties. Aluminum possesses a high thermal conductivity (λ) of approximately 237 W/m·K [20], which ensures efficient heat distribution and a uniform surface temperature. This characteristic allows temperature measurements taken at a single point using a thermocouple to accurately represent the overall surface temperature. In addition, aluminum exhibits high thermal diffusivity (α) (≈97.1 × 10^{-6} m^2/s [20]), enabling rapid absorption and release of heat in response to environmental changes. Consequently, the substrate temperature responds quickly to variations in solar irradiation, such as when sunlight is intermittently blocked by clouds, ensuring reliable and dynamic measurement of radiative cooling performance.

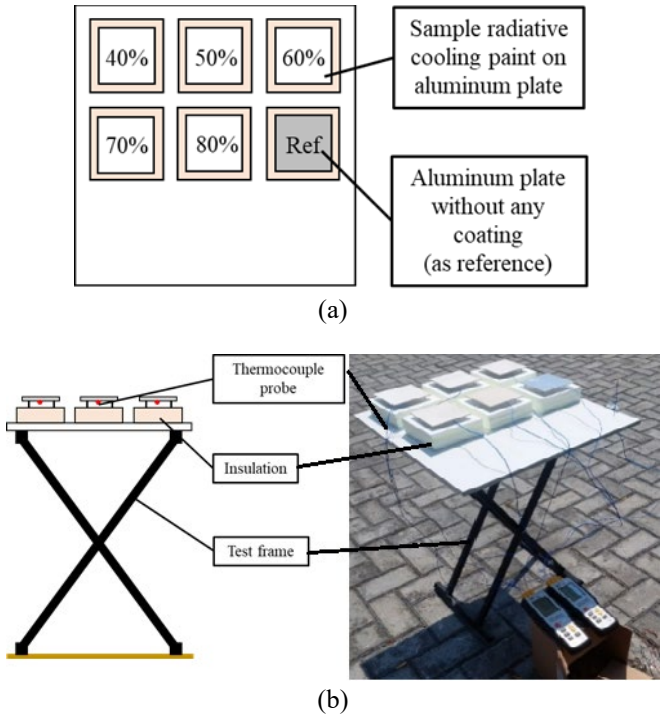

Figure 4. Test setup for optimal pigment volume concentration (PVC): (a) top view and (b) side view

Five identical tests were conducted, each corresponding to one of the five pigment types. All tests took place under natural sunlight between 09:30 and 14:30 local time, when solar irradiation was at its peak. The experiments were carried out in an open area located in Sumedang, West Java, Indonesia. The ambient temperature (Tamb) was approximately 27–30 °C during November 2024. Figure 4 illustrates the experimental setup. For each pigment type, five aluminum plates were coated with RCP formulations at different PVCs of 40%, 50%, 60%, 70%, and 80%. These plates were prepared and tested simultaneously. The backside of each plate was thermally insulated to minimize heat transfer by conduction from the supporting surface. One uncoated aluminum plate was also included as a reference sample to compare the cooling performance of the coatings with that of bare aluminum.

During testing, the backside surface temperature of each plate was recorded at five-minute intervals. Thermocouples were attached to the center of each sample. The temperature of the uncoated plate served as the baseline reference. The collected temperature data were processed to calculate the average temperature decrease (ΔT) achieved by each RCP sample according to Eq. (2).

$$\Delta T_{Avg} = \frac{1}{n} \sum_{i=1}^{n} (T_{With\ RCP,i} - T_{Without\ RCP,i}), \quad (2)$$

where, ΔT_{Avg} is the average temperature decrease, n is the number of temperature measurements, and T is the temperature of the backside surface of the aluminum plate. The average temperature decrease was summarized with the previous observations regarding the presence or absence of cracks in the RCP layer after drying for all RCP samples with five types of pigments and five variations in PVC. The optimal PVC for each pigment type was established based on the absence of cracks and the highest average temperature decrease.

3. RESULTS AND DISCUSSION

In this section, a result report related to crack occurrences and the decrease in temperature performance will be presented.

3.1 Crack phenomenon

Based on visual observations, the occurrence of surface cracking in the RCP layers for all five pigment types and five PVC variations is summarized in Table 2.

Table 2. Occurrence of cracks in RCP after drying (×: no crack, ✓: crack)

Pigment	Pigment Volume Concentration (PVC)				
	40%	50%	60%	70%	80%
$CaCO_3$	×	×	×	×	✓
$BaSO_4$	×	×	×	✓	✓
MgO	×	×	×	×	×
TiO_2	×	×	×	✓	✓
SiO_2	×	×	✓	✓	✓

The visual inspection results of the RCP coatings are summarised in Table 2. Cracking was observed to occur predominantly at higher PVC levels, particularly at 70% and 80%. This was except for MgO-based coatings, which showed no visible cracking at any concentration. The $CaCO_3$ and $BaSO_4$ coatings began to exhibit cracking at 80% and 70% PVC, respectively. TiO_2 and SiO_2 coatings displayed cracks starting at 60% and 70%, respectively. These findings indicate that excessive pigment concentration reduces the binder content. This results in insufficient matrix support for the pigment particles and reduced coating flexibility. Conversely, MgO exhibited superior structural stability, likely due to its smaller particle size and stronger interfacial interaction with the PMMA binder. This enhanced mechanical integrity even at higher PVC levels.

This tendency for cracking is supported by existing research. Cracking in RCP layers generally occurs when the amount of binder is insufficient to form a continuous and flexible matrix for the pigment particles, particularly at high PVC levels [10]. The study by Rodríguez [21] investigates how varying the PVC relative to the critical PVC CPVC affects the thermal and mechanical behaviour of epoxy coatings. Coatings remain relatively uniform and mechanically stable when PVC is below CPVC. They become porous and structurally compromised once PVC exceeds this threshold. As the PVC increases, the binder content decreases. This results in a coating that is stiffer, more brittle, and less capable of accommodating internal stresses. These findings directly support the principle that increasing PVC diminishes the continuous binder matrix. The film transitions from a tough, cohesive structure into a more rigid and fragile one, ultimately degrading its overall mechanical resilience.

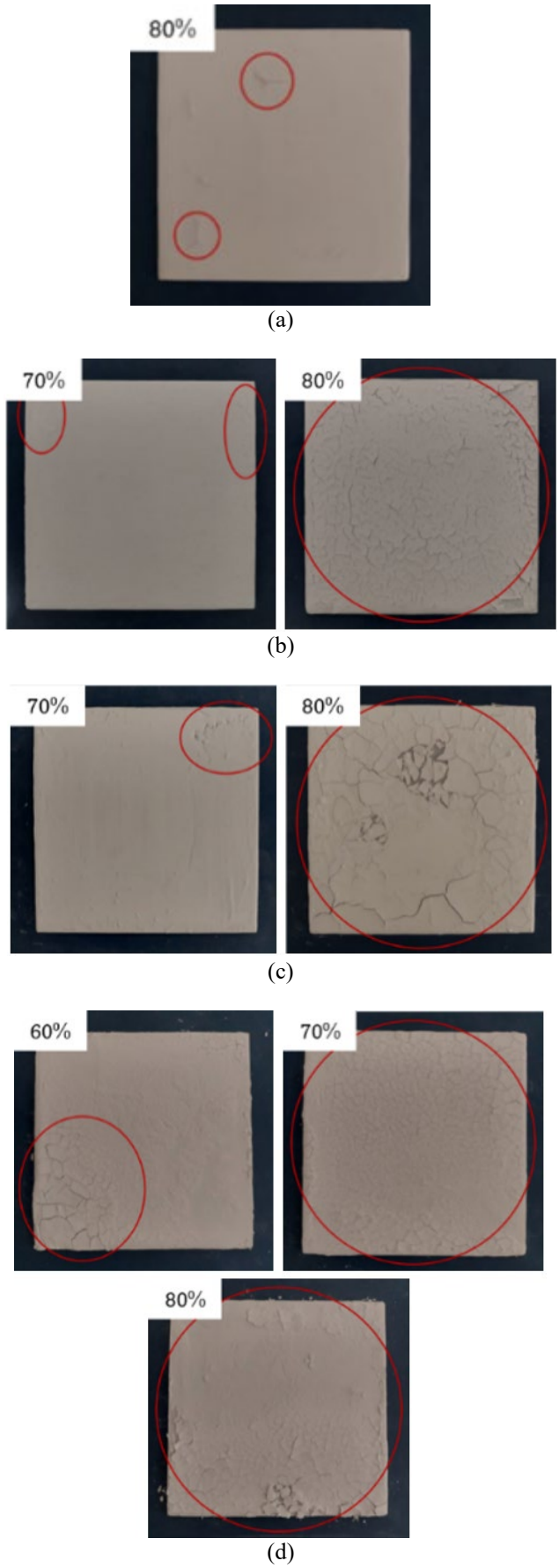

Figure 5. Crack occurrences based on pigment materials and concentrations: a) $CaCO_3$, b) $BaSO_4$, c) TiO_2, d) SiO_2

During the drying process, solvent evaporation induces shrinkage within the coating layer. Without an adequate amount of binder to absorb and distribute the stresses caused by shrinkage, tensile forces develop that exceed the mechanical strength of the weakened film, resulting in cracks forming. The specific locations where surface cracking occurred for each pigment type and PVC level are illustrated in Figure 5, with red circles marking the cracked regions.

The PVC level at which cracking first appears varies among pigment types due to several interrelated material properties. Pigment density is one of the most influential factors. A higher pigment density increases the pigment mass fraction relative to the binder. This reduces the amount of binder available for matrix formation. For instance, calcium carbonate ($CaCO_3$) has a relatively low density (2.8 g/mL). This allowed the coating to remain intact up to 80% PVC. In contrast, barium sulfate ($BaSO_4$, 4.5 g/mL) and titanium dioxide (TiO_2, 4.3 g/mL) exhibited cracking at 70% PVC. Their higher densities led to lower binder content at equivalent PVCs. Interestingly, magnesium oxide (MgO) coatings showed no visible cracking across all PVC levels, despite MgO's relatively high density (3.6 g/mL). This anomaly may be attributed to the impurity content (approximately 10%) in the MgO pigment used. These impurities may have altered the microstructure of the coating, thereby improving stress distribution and enhancing crack resistance. Such impurities may have acted as fillers, improving particle packing and reducing internal stress concentrations within the layer.

For silicon dioxide (SiO_2), cracking appeared at a much lower PVC (60%). This can be attributed to its large particle size (approximately 100 μm) compared to that of TiO_2 (around 0.3 μm). Research by Cardell et al. [22] shows that the size of pigment particles has a dramatic influence on how paint behaves and degrades. Coarse particles tend to accumulate binder in the interparticle voids, leading to more severe crack formation upon ageing. Finer particles more strongly alter the binder structure and cause more rapid colour changes. Larger particles tend to create voids and weak interparticle bonding within the matrix. This results in higher internal stresses during solvent evaporation and greater susceptibility to cracking. In contrast, smaller pigment particles contribute to more uniform packing, improved binder adhesion, and better mechanical integrity. Therefore, both density and particle size play critical roles in determining the mechanical stability of RCP coatings at varying pigment concentrations.

3.2 Performance of decreasing temperature

The experimental results for the backside surface temperature of aluminum plates coated with RCP using five different pigments and five PVC variations are presented in Figure 6. Here, the type of pigment determines the coating's ability to reflect and emit heat, while the variation in PVC influences the concentration of pigment within the binder, affecting both optical properties and physical structure. The corresponding temperature of the uncoated aluminum plate, referred to as "Ref," serves as the baseline reference for evaluating the thermal performance of the coated samples. This comparison enables assessment of how both pigment and PVC level influence the coating's heat reflectance characteristics.

Figure 6 summarizes the experimental evaluation of RCV using five pigment materials: calcium carbonate ($CaCO_3$), barium sulfate ($BaSO_4$), magnesium oxide (MgO), titanium dioxide (TiO_2), and silicon dioxide (SiO_2). It details temperature measurements at the backside surface of aluminum plates coated with each RCP formulation, forming the basis for assessing the influence of pigment type and PVC on thermal performance and cooling efficiency. This information is crucial to understanding how pigment composition affects radiative emissivity, solar reflectance, and resultant surface temperature reduction under direct sunlight, consistent with approaches by Raman et al. [23] and Mandal et al. [24].

The use of aluminum substrates for all tests ensures uniformity in thermal conduction, allowing for an accurate comparison of coating performance. The inclusion of multiple pigment types represents a deliberate effort to explore variations in optical and thermal behavior across materials with differing refractive indices, densities, and particle morphologies. Such an approach aligns with prior findings that highlight the significance of pigment selection and concentration in determining the balance between cooling efficiency and mechanical durability of radiative coatings [25-27]. Overall, Figure 6 provides the empirical foundation necessary to identify the optimal PVC for each pigment type, supporting advancements in passive cooling materials for energy-efficient surface coatings.

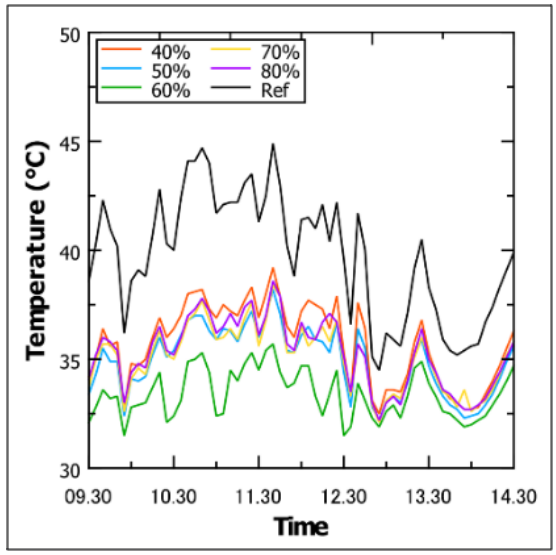

(a)

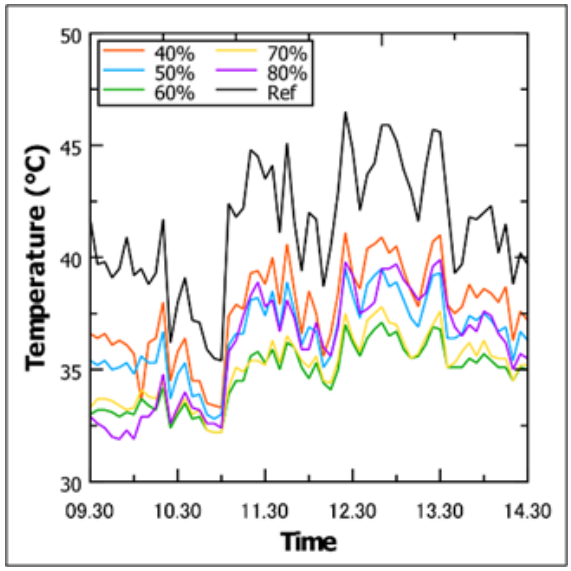

(b)

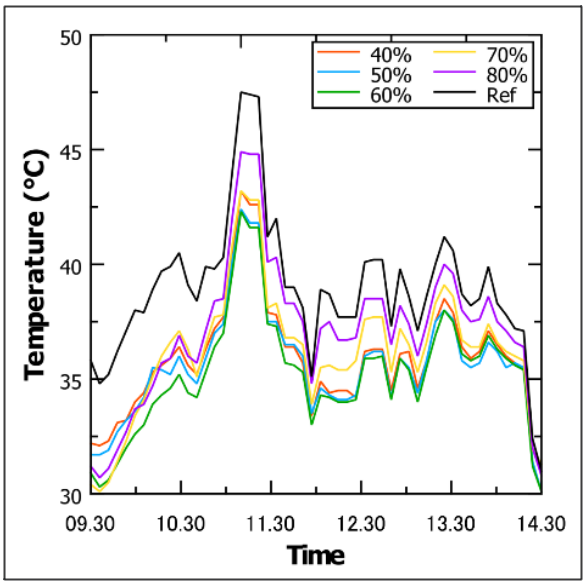

(c)

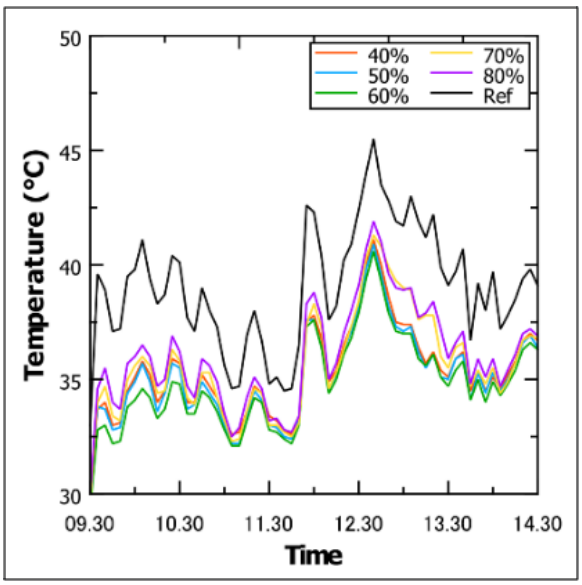

(d)

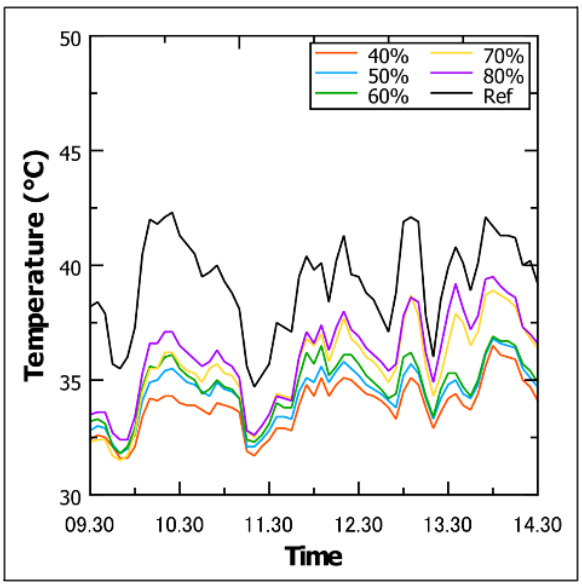

(e)

Figure 6. Temperature profile on alumnium surface for each pigment: a) $CaCO_3$, b) $BaSO_4$, c) MgO, d) TiO_2, e) SiO_2

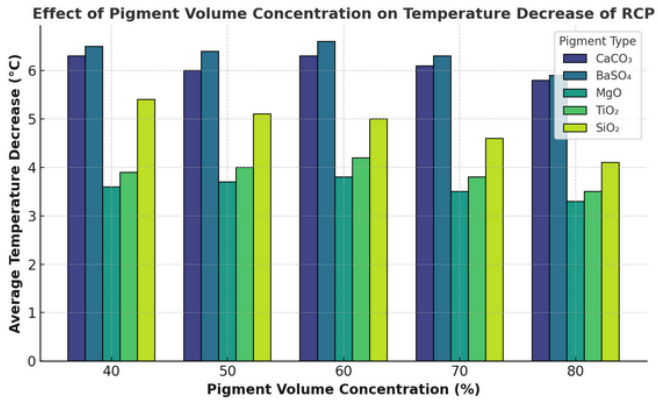

Figure 7. Average temperature decrease for each different type of pigment material and concentration

For the $CaCO_3$, $BaSO_4$, MgO, and TiO_2 pigments, the relationship between PVC and average temperature decrease shows a hill-shaped trend. This is illustrated by the green, blue, yellow, and gray bars in Figure 7, respectively. The maximum cooling performance for these pigments occurred at a PVC of 60%. At lower PVCs (40% and 50%), the temperature decrease was reduced. This resulted from an insufficient number of pigment particles within the RCP layer, which limited the coating's solar reflectivity and infrared emissivity. As a result, the radiative cooling effect was weakened. In contrast, increasing the PVC beyond 60% (to 70% and 80%) did not enhance the cooling performance, even with higher pigment content. This behavior is due to two main factors. First, surface cracking occurred at high PVCs, creating discontinuities in the coating that exposed the aluminum substrate to direct solar radiation. Second, the reduction in binder content at high PVCs caused particle crowding. Densely packed pigment particles limited light scattering and disrupted the uniform optical path within the coating [28].

Particle crowding has been shown to greatly reduce scattering efficiency in radiative cooling materials [29]. This results in decreased solar reflectance and increased absorption of incident radiation by the substrate. This mechanism explains why the $CaCO_3$ and MgO coatings exhibited lower temperature decreases at 70% PVC compared to 60%, even when no visible cracks were observed. The crowding effect counteracted the potential benefits of increased pigment loading.

In contrast, the SiO_2 pigment displayed a monotonically decreasing, staircase-like trend in average temperature decrease. This is shown by the red bars in Figure 7. The highest temperature reduction for SiO_2-based RCP was achieved at 40% PVC, with performance declining as PVC increased. The onset of crowding, observed from 50% PVC onward, is attributed to the large particle size of SiO_2. This restricts uniform packing and reduces the coating's optical scattering efficiency. Considering both mechanical integrity and thermal performance, the optimal PVC values were found to be 60% for $CaCO_3$, $BaSO_4$, MgO, and TiO_2, and 40% for SiO_2. At these concentrations, the RCP layers showed no cracking and achieved the highest average temperature decreases, as indicated by the green-highlighted results in Table 3. These findings underscore the importance of balancing pigment loading with binder content to achieve optimal radiative cooling performance and structural stability in RCP coatings.

Table 3. Recapitulation of average temperature decrease and crack occurrence (✕: no crack, ✓: crack)

Pigment	Average Temperature Decrease/ Crack Occurrence				
	PVC 40%	PVC 50%	PVC 60%	PVC 70%	PVC 80%
$CaCO_3$	4.0 °C ✕	4.8 °C ✕	6.3 °C ✕	4.6 °C ✕	4.5 °C ✓
$BaSO_4$	3.7 °C ✕	4.8 °C ✕	6.6 °C ✕	6.3 °C ✓	5.3 °C ✓
MgO	3.1 °C ✕	3.3 °C ✕	3.8 °C ✕	2.7 °C ✕	1.9 °C ✕
TiO_2	3.7 °C ✕	3.9 °C ✕	4.2 °C ✕	3.4 °C ✓	3.0 °C ✓
SiO_2	5.4 °C ✕	4.8 °C ✕	4.5 °C ✓	3.7 °C ✓	3.1 °C ✓

4. FUTURE STUDY

Although the present analysis provides important insights into how PVC, pigment particle size, and binder–pigment interactions influence coating stiffness, brittleness, void formation, and cracking susceptibility, several key areas remain open for future investigation. First, the long-term durability of the coating has not been assessed, particularly under realistic environmental stressors such as prolonged sunlight exposure, rain, humidity fluctuations, and thermal cycling. These conditions are known to accelerate polymer oxidation, promote microcrack development, and alter coating adhesion over time [30, 31]. Understanding how coatings with varying PVC and particle-size distributions evolve under such conditions will be critical for predicting field performance, especially because larger particles and coatings above CPVC may accumulate internal stresses that worsen during environmental aging.

Second, further research is needed to determine the water resistance and barrier properties of the formulations. Higher PVC and larger pigment particles have been associated with increased void content and reduced binder continuity, which may elevate water absorption and permeability [32, 33] Evaluating parameters such as water uptake, vapor permeability, salt-spray resistance, and electrochemical impedance spectroscopy (EIS) performance would provide a more complete understanding of how microstructural features, such as weak interparticle bonds and voids translate to real-world protective capability. This is particularly relevant for coatings intended for outdoor or corrosive environments.

Finally, the scalability and practical feasibility of the coating preparation method should be addressed. Laboratory-scale formulations often rely on controlled dispersion, slow curing, or specific mixing protocols that may not translate easily to industry. Variables such as rheology behavior during large-batch mixing, pigment dispersion energy, coating uniformity during application, and drying time under industrial conditions should be examined.

Additionally, the influence of pigment size and PVC on processability, such as sedimentation, viscosity stability, and film leveling, should be considered, as void-forming large particles in PVC systems may present manufacturing or application limitations. Addressing these gaps will enhance the practical relevance of the current findings and support the development of high-performance, durable coatings that strike a balance between mechanical integrity, environmental resistance, and manufacturability.

5. CONCLUSIONS

The optimal PVC for each RCP was determined using two criteria. First, there had to be no surface cracking in the RCP layer after drying. Second, the paint needed to achieve the highest temperature decrease when exposed to direct sunlight. Twenty-five RCP samples were prepared, consisting of five pigment types ($CaCO_3$, $BaSO_4$, MgO, TiO_2, SiO_2) with five PVC levels (40%, 50%, 60%, 70%, 80%), all applied to aluminium.

For the $CaCO_3$-based RCP, only 80% PVC showed cracking. The maximum temperature decrease, 6.3 °C, was at 60% PVC. For $BaSO_4$-based RCP, cracking occurred at 70% and 80% PVC, while the optimal cooling, 6.6 °C, was achieved at 60% PVC. The MgO-based RCP showed no visible cracking at any PVC. Its maximum temperature decrease, 3.8 °C, also occurred at a 60% PVC content. TiO_2-based RCP cracked at 70% and 80% PVC, with the highest decrease, 4.2 °C, at 60% PVC. SiO_2-based RCP exhibited cracking at 60% PVC and above. The highest decrease for SiO_2, 5.4 °C, was at 40% PVC.

The optimal PVC was 60% for $CaCO_3$, $BaSO_4$, MgO, and TiO_2, and 40% for SiO_2. These concentrations strike a balance between high pigment loading for reflectivity and sufficient binder to prevent cracking. The results show that careful PVC tuning is critical for high-performance RCP coatings that optimise both cooling and mechanical stability. Each pigment has a specific PVC limit above which integrity suffers. Formulation should target PVC values below this cracking threshold. This approach maintains stability while enhancing reflectivity and emissivity. Careful PVC tuning is key for durable, high-performance RCPs in real environments.

ACKNOWLEDGMENT

This work was supported by the Institute of Research and Community Service (Lembaga Penelitian dan Pengabdian Masyarakat, LPPM) and the Department of Mechanical Engineering, Institut Teknologi Nasional Bandung (ITENAS), Bandung, Indonesia.

REFERENCES

[1] Lundgren-Kownacki, K., Hornyanszky, E.D., Chu, T.A., Olsson, J.A., Becker, P. (2018). Challenges of using air conditioning in an increasingly hot climate. International Journal of Biometeorology, 62(3): 401-412. https://doi.org/10.1007/s00484-017-1493-z

[2] Dwivedi, P., Sudhakar, K., Soni, A., Solomin, E., Kirpichnikova, I. (2020). Advanced cooling techniques of P.V. modules: A state of art. Case Study of Thermal Engineering, 21: 100674. https://doi.org/10.1016/j.csite.2020.100674

[3] Silva, R., Eggimann, S., Fierz, L., Fiorentini, M., Orehounig, K., Baldini, L. (2002). Opportunities for passive cooling to mitigate the impact of climate change in Switzerland. Building and Environment, 208: 108574. https://doi.org/10.1016/j.buildenv.2021.108574

[4] Ahmed, A., Garcia, M.M., McGough, D., Caratella, K., Ure, Z. (2018). Experimental evaluation of passive

cooling using phase change material (PCM) for reducing overheating in public building. E3S Web of Conferences 32: 01001. https://doi.org/10.1051/e3sconf/20183201001

[5] Zahid, I., Qamar, A., Farooq, M., Riaz, F., Habib, M.S., Farhan, M., Sultan, M., Rehman, A.U., Hayat, M.A. (2023). Experimental optimization of various heat sinks using passive thermal management system. Case Study Thermal Engineering, 49: 103262. https://doi.org/10.1016/j.csite.2023.103262

[6] Chang, K., Wang, Y.Y., Li, Y.Z. (2023). A review of water sublimation cooling and water evaporation cooling in complex space environments. Progress in Aerospace Sciences, 140: 100930. https://doi.org/10.1016/j.paerosci.2023.100930

[7] Liang, L., Bai, S., Lin, K., Kwok, C.T., Chen, S., Zhu, Y., Tso, C.Y. (2024). Advancing sustainable development: Broad applications of passive radiative cooling. Sustainability, 16(6): 2346. https://doi.org/10.3390/su16062346

[8] Mandal, J., Yang, Y., Yu, N., Raman, A.P. (2020). Paints as a scalable and effective radiative cooling technology for buildings. Joule, 4(7): 1350-1356. https://doi.org/10.1016/j.joule.2020.04.010

[9] Atiganyanun, S., Kumnorkaew, P. (2023). Effects of pigment volume concentration on radiative cooling properties of acrylic-based paints with calcium carbonate and hollow silicon dioxide microparticles. International Journal of Sustainable Energy, 42(1): 612-626. https://doi.org/10.1080/14786451.2023.2221082

[10] Rooney, M.T. (2018). Effect of pigment volume concentration on physical and chemical properties of acrylic emulsion paints assessed using single-sided NMR. The College of William & Mary, Williamsburg. https://doi.org/10.21220/s2-7g4k-fr37

[11] Lim, H., Chae, D., Son, S., Ju, S., Ha, J., Lee, H. (2021). Sub-ambient radiative cooling realized using CaCO3 microparticle-based single layer without metal refector for entire day. Research Square. https://doi.org/10.21203/rs.3.rs-523745/v1

[12] Li, X., Peoples, J., Huang, Z., Zhao, Z., Qiu, J., Ruan, X. (2020). Full daytime sub-ambient radiative cooling in commercial-like paints with high figure of merit. Cell Reports Physal Science, 1(10): 100221. https://doi.org/10.1016/j.xcrp.2020.100221

[13] Joseph, W.R., Tan, J.Y., Koyande, A.K., Khoiroh, I., Joynson, J., Willis, S. (2023). Subambient passive radiative cooling effects of barium sulfate and calcium carbonate paints under Malaysia's tropical climate. Environmental Advance Science, 2(12): 1662-1679. https://doi.org/10.1039/D3VA00161J

[14] Li, X., Peoples, J., Yao, P., Ruan, X. (2021). Ultrawhite $BaSO_4$ paints and films for remarkable daytime subambient radiative cooling, ACS applied. Mater Interfaces, 13(18): 21733-21739. https://doi.org/10.1021/acsami.1c02368

[15] Felicelli, A., Wang, J., Feng, D., Forti, E., Azrak, S.E.A., Peoples, J., Youngblood, J., Chiu, G., Ruan, X. (2024). Efficient radiative cooling of low-cost $BaSO_4$ paint-paper dual-layer thin films. Nanophotonics, 13(5): 639-648. https://doi.org/10.1515/nanoph-2023-0642

[16] Das, P., Rudra, S., Maurya, K.C., Saha, B. (2023). Ultra-emissive MgO-PVDF polymer nanocomposite paint for passive daytime radiative cooling. Advance Material Technology, 8(24): 2301174. https://doi.org/10.1002/admt.202301174

[17] Altamimi, M.M.S., Saeed, U., Al-Turaif, H. (2023). BaSO4/TiO2 microparticle embedded in polyvinylidene fluoride-co-hexafluoropropylene/ polytetrafluoroethylene polymer film for daytime radiative cooling. Polymers (Basel), 15(19): 3876. https://doi.org/10.3390/polym15193876

[18] Mishra, B.R., Sundaram, S., Sasihithlu, K. (2024). Design of Radiative cooling paint coating and insights into its sub-ambient cooling behaviour. ArXiv Prepr. https://doi.org/10.48550/arXiv.2401.11765

[19] Putra, D.F.A., Qazi, U., Chen, P.H., Shih, S.J. (2024). Preparation and characterization of SiO2-PMMA and TiO2-SiO2-PMMA composite thick films for radiative cooling application. Journal of Compos Science, 8(11): 453. https://doi.org/10.3390/jcs8110453

[20] Bergman, T.L., Lavine, A.S., Incropera, F.P., Dewitt, D.P. (2011). Fundamentals of Heat and Mass Transfer, Seventh Ed. John Wiley & Sons, Inc.

[21] Rodríguez, M. (2024). The influence of pigment volume concentration (PVC) on the properties of an epoxy coating Part I. Thermal and mechanical properties. Progress Organic Coatings, 50(1): 62-67. https://doi.org/10.1016/j.porgcoat.2003.10.013

[22] Cardell, C., Herrera, A., Guerra, I., Navas, N., Rodríguez Simón, L., Elert, K. (2017). Pigment-size effect on the physico-chemical behavior of azurite-tempera dosimeters upon natural and accelerated photo aging. Dyes and Pigments, 141: 53-65. https://doi.org/10.1016/j.dyepig.2017.02.001

[23] Raman, A.P., Anoma, M.A., Zhu, L., Rephaeli, E., Fan, S. (2014). Passive radiative cooling below ambient air temperature under direct sunlight. Nature, 515(7528): 540-544. https://doi.org/10.1038/nature13883

[24] Mandal, J., Fu, Y., Overvig, A.C., Jia, M., Sun, K., Shi, N.N., Zhou, H., Xiao, X., Yu, N., Yang, Y. (2018). Hierarchically porous polymer coatings for highly efficient passive daytime radiative cooling. Science, 362(6412): 315-319. https://doi.org/10.1126/science.aat9513

[25] Zhai, Y., Ma, Y., David, S.N., Zhao, D., Lou, R., Tan, G., Yang, R., Yin, X. (2017). Scalable-manufactured randomized glass–polymer hybrid metamaterial for daytime radiative cooling. Science, 355(6329): 1062-1066. https://doi.org/10.1126/science.aai7899

[26] Kou, J., Jurado, Z., Chen, Z., Fan, S., Minnich, A.J. (2017). Daytime radiative cooling using near-black infrared emitters. ACS Photonics, 4(3): 626-630. https://doi.org/10.1021/acsphotonics.6b00991

[27] Zhao, D., Aili, A., Zhai, Y., Lu, J., Kidd, D., Tan, G., Yin, X., Yang, R. (2019). Subambient cooling of water: Toward real-world applications of daytime radiative cooling. Joule, 3(1): 111-123. https://doi.org/10.1016/j.joule.2018.10.006

[28] Brown, R.F.G., Carr, C., Taylor, M.E. (1997). Effect of pigment volume concentration and latex particle size on pigment distribution. Progress Organic Coatings, 30(3): 185-194. https://doi.org/10.1016/S0300-9440(96)00686-8

[29] Lan, Y.X., Chen, Y.H., Chao, Y.L., Chang, Y.H., Huang, Y.C., Liu, W.R., Wong, W.T., Sun, A.C.F., Santiago, K.S., Yeh, J.M. (2024). Green and heavy-duty anticorrosion coatings: Waterborne epoxy thermoset

composites modified through variation of zinc dust loading and incorporation of amine-capped aniline trimer and graphene oxide. Polymers, 16(9): 1252. https://doi.org/10.3390/polym16091252
[30] Zargarnezhad, H., Wong, D., Catherine Lam, C.N., Asselin, E. (2024). Long-term performance of epoxy-based coatings: Hydrothermal exposure. Progress in Organic Coatings, 196: 108697. https://doi.org/10.1016/j.porgcoat.2024.108697
[31] Sabet-Bokati, K., Bakhshandeh, E., Russell, Z., Gaier, M., Plucknett, K.P. (2025). Critical investigation of the long-term integrity of sustainable anti-corrosion coatings in static and dynamic humid environments. Progress in Organic Coatings, 204: 109276. https://doi.org/10.1016/j.porgcoat.2025.109276
[32] Funke, W. (1997). Problems and progress in organic coatings science and technology. Progress in Organic Coatings, 31(1-2): 5-9. https://doi.org/10.1016/S0300-9440(97)00013-1
[33] Wicks, Z.W., Jones, F.N., Pappas, S.P., Wicks, D.A. (2007). Organic Coatings: Science and Technology. John Wiley & Sons Inc., Hoboken. http://doi.org/10.1002/047007907X

NOMENCLATURE

AC	air conditioner
DMF	dimethyl formamide
PCM	phase change materials
PVC	pigment volume concentration
PMMA	polymethyl methacrylate
RCP	Radiative cooling paint

Greek symbols

λ	thermal conductivity, $W \cdot m^{-1} K^{-1}$
α	thermal diffusivity, $m^2 \cdot s^{-1}$
β	thermal expansion coefficient, K^{-1}
Δ	differency
m	mass, kg
P	Density, $kg \cdot m^{-3}$
T	Temperature, °C

Subscript

avg	average
P	mass of pigment
B	mass of Binder
ambient	ambient